Fusion Engineering and Design 135 (2018) 81–87

Contents lists available at ScienceDirect

Fusion Engineering and Design

journal homepage: www.elsevier.com/locate/fusengdes

A distillation column for hydrogen isotope removal from liquid lithium

M. Christenson*, C. Moynihan, D.N. Ruzic

Center for Plasma-Materials Interactions, 201 South Goodwin Avenue, Urbana, IL 61801, United States

ARTICLE INFO

Keywords:
Plasma-facing component
Lithium
Tritium
Recovery
Reclamation
Distillation

ABSTRACT

Recovery of tritium from plasma-facing components in fusion devices will be vital to future full-scale operation. Liquid, low-Z materials have demonstrated many inherent advantages over solid first wall materials. To this end, a thermal treatment method in the form of a distillation column for extraction of hydrogen isotopes from liquid lithium has been designed, developed, and constructed at the Center for Plasma-Material Interactions at the University of Illinois at Urbana-Champaign. Use of induction heating and lithium condensation stages are the two qualities that set this design apart from other thermal treatment systems. Induction heating capabilities were modeled using the COMSOL Multiphysics software, which were validated when commissioning the physical heater module. Proof-of-concept tests were performed in the prototype column, which were undertaken as batch processes to investigate the efficacy with which the column could remove hydrogen gas from lithium-rich and lithium hydride-rich samples. All of the tests reported used lithium hydride as a surrogate for lithium deuteride and lithium tritide. The design process and results from the initial tests will be discussed, along with the envisioned placement of this treatment scheme in a fully-functional lithium loop.

1. Introduction

As lithium has gained popularity in the fusion community as an alternative wall material due to its ability to enhance confinement [1] and consume impurity and cold fuel particles [2], it has become clear that the biggest roadblock to the universal application of lithium (Li) as a first wall material is its ability to retain tritium (T). These concerns exist because on-site tritium inventory is limited due to availability and radiation safety [3].

Due to these concerns, various methods [4–7] have been proposed with the sole purpose of separating tritium from lithium and lithium alloys. Catalytic separation using yttrium has been studied in the context of the Internal Fusion Materials Irradiation Facility (IFMIF) lithium loop [4], but appears to suffer from low tritium yields. The combination of molten salt extraction and electrolysis [6] has demonstrated the ability to evolve tritium at rates that approach reactor-relevant operation; however, yields from this process are still too low, and the technology itself suffers from the presence of impurities and the production of unwanted by-products. The most promising techniques for recovering tritium from lithium are those that take advantage of the thermophysical properties of the lithium-lithium hydride (lithium deuteride, lithium tritide) phases, such as those proposed in Ref. [7]. What is noticeably absent from these systems is a way to actually evolve tritium and deuterium gas from lithium solutions. This absence was the primary motivator for the work accomplished at the University of Illinois.

To fill in this missing step, specifically with regards to the loop system proposed in Ono's work [7], a distillation column for hydrogen isotope evolution from lithium was designed, developed, constructed, and tested at the Center for Plasma-Material Interactions [8]. Two components of this design set it apart from other conventional distillation columns. First, induction heating was used as the primary driver for evolution, since induction drive heats metals more rapidly. The induction heating capabilities were modeled in the COMSOL Multiphysics simulation software [9].The accuracy of the simulation was verified with a commissioning test, where the working coil was used to heat the actual column structure. Second, condensation stages were built into the column to capture lithium vapor. These stages, and an evaluation of how much lithium was able to travel up and through the column, were based on the work done by Goldston [10] on the Lithium Vapor Box Divertor.

Proof-of-concept tests were then performed in the fully-constructed, prototype distillation column. These tests were conducted with samples having various hydrogen molar ratios in mixtures that contained both lithium (Li) and lithium hydride (LiH). The effectiveness of the column at removing hydrogen was then gauged by monitoring the partial pressures as the “bucket” of the column was heated using the induction heater. The results from these tests will be described later; however, one

* Corresponding author.
E-mail addresses: mpchris2@illinois.edu (M. Christenson), cmoynih2@illinois.edu (C. Moynihan).

https://doi.org/10.1016/j.fusengdes.2018.07.009
Received 14 April 2018; Received in revised form 22 June 2018; Accepted 11 July 2018
Available online 26 July 2018

of the more important conclusions that was drawn was that the hydrogen concentration in the lithium sample was pivotal to the resultant evolution rate.

This paper presents the design, development, and operation of the prototype distillation column constructed at the Center for Plasma-Material Interactions (CPMI) to recover hydrogen gas from hydrogenated lithium samples. The thermodynamics and kinetics which govern hydrogen release in this system have also been thoroughly explored at CPMI at smaller scales. Section 2 describes the theory and design criteria used for the column development. This includes the simulation of the induction heating capabilities of the actual source. Section 3 presents the results from the commissioning and Proof-of-concept tests, wherein a lithium-rich and a lithium hydride-rich sample were tested. Section 4 discusses the impact of the results from this prototype technology, and what these results mean within the context of larger liquid lithium loop systems. Section 5 summarizes the results and describes future experimental work.

2. Theory and design

The prototype distillation column was designed to extract hydrogen from batch lithium melts and collect the evaporated lithium. Two novelties of design seek to accomplish these goals: inclined condensation stages and induction heating. Induction heating is the driving force behind hydrogen desorption and was modeled using the COMSOL® Multiphysics software. Clean lithium collection and potential diversion occur at the condensation stages. Lithium flow is analyzed through a mass and energy balance. Design considerations allow for safe operation, efficiency, and future extensions.

2.1. Column

Induction heating drives thermal desorption of hydrogen in the lithium melt. As temperatures increase, hydrogen and lithium vapor flow upward and encounter the first condensation stage (Fig. 1a), which is kept at 315 °C to allow for lithium condensation but limit hydrogen co-deposition [11]. Hydrogen is then directed toward a small outlet into the second condensation section, creating nozzled flow. The second condensation stage works to condense more of the lithium vapor and funnel the hydrogen towards the top of the chamber. The hydrogen reaches a small aperture (1.14 mm) that restricts the flow of hydrogen into the region of the chamber containing the residual gas analyzer (RGA). As the hydrogen exits the top of the column, it could be directed towards gas separation technologies and eventually back into the reactor.

The condensation stages are the key feature for lithium collection. The upward angle of 45° and temperatures above lithium's melting temperature allow for flow of lithium back down toward the bucket. In the proposed loop system, the flow of lithium off of the stages could be used to recycle clean lithium back to the in-vessel, plasma-material interface. Each stage is connected to the rest of the column by two set screws, making the stages completely modular. Stages could be removed or added to meet the specifications of the system. Stages can also be manufactured readily, such that an array of distillation columns would be easily attainable. Buildup of hydrogen inside the chamber could be a concern. However, the gas relief lip (Fig. 1b) allows for flow of gas to the portion of the chamber outside the column walls, where it can be pumped out, preventing this buildup. The bucket (Fig. 1b) is grooved to prevent warping during the rapid rise in temperature during operation. The bucket was welded into an 203 mm ConFlat flange to allow easy attachment to the vacuum chamber.

2.2. COMSOL heating

The presence of solid hydrides in lithium melts requires temperatures near 690 °C, the melting temperature of lithium hydride, to promote thermal desorption of hydrogen. Near these temperatures, the solid hydride precipitate, known as the β phase, dissolves into solution into what is known as the α phase. This type of chemistry has been observed in lithium-lithium hydride systems [8,12,13], and is the fundamental principal which governs hydrogen isotope recovery from thermal treatment systems. This is of particular importance when no hydrogen originally exists in the mixture in the α phase. As such, treatment temperatures near the melting point of lithium hydride are necessary for appreciable recovery.

Induction heating's efficiency at heating metals gives it a distinct advantage over the use of resistive heating. COMSOL Multiphysics® was used to model the induction heating of the column's lower bucket [9]. The induction heating module is based on the coupling of heat transfer in solids, Lenz's Law, and Ampere's Law. Induction heating uses a coil carrying high frequency current to create alternating magnetic fields in the workpiece. These alternating fields create eddy currents, which heat the workpiece through Ohmic dissipation. Changes in resistivity throughout heating require the physics to be coupled, such that these changes can inform the rest of the physics.

The physics is based on three fundamental equations, the thermal energy equation for heat transfer in solids and a combination of Lenz's Law and Ampere's Law [9]:

$$\rho C_p \frac{\partial T}{\partial t} + \rho C_p \mathbf{u}\cdot\nabla T = \nabla\cdot(k\nabla T) + Q, \tag{1}$$

$$(i\omega\sigma - \omega^2\epsilon_0\epsilon_r)\mathbf{A} + \nabla\times\frac{\mathbf{B}}{\mu_0\mu_r} - \sigma\mathbf{v}\times\mathbf{B} = \mathbf{J}_e, \tag{2}$$

$$\mathbf{B} = \nabla\times\mathbf{A}, \tag{3}$$

where ρ is the material density, C_p is the constant-pressure heat capacity of the material, T is the temperature of the material in K, $\mathbf{u}$ is the advection term for the thermal energy equation, k is the heat conductivity of the material, Q is the heat source, i is the imaginary root, ω is the angular frequency at which the induction coil is driven, $\epsilon_0\epsilon_r$ is the product of the permittivity of free space and that of the specific material, $\mathbf{A}$ is the magnetic vector potential defined by Eq. (3), $\mathbf{B}$ is the magnetic field, $\mu_0\mu_r$ is the product of the permeability in vacuum and in the specific material, σ is the electrical conductivity of the material, $\mathbf{v}$ is the velocity vector, and $\mathbf{J}_e$ is the current driven in the material. The coupling of the physics is in the heat source term [9]:

$$Q = \frac{1}{2}\mathrm{Re}(\mathbf{J}\cdot\mathbf{E}^*) + \frac{1}{2}\mathrm{Re}(i\omega\mathbf{B}\cdot\mathbf{H}^*), \tag{4}$$

where $\mathbf{J}$ is the total current, $\mathbf{E}^*$ is the complex conjugate of the electric field, $\mathbf{B}$ is the magnetic field, and $\mathbf{H}^*$ is the complex conjugate of the auxiliary field.

The COMSOL model was constructed as a 2-dimensional axisymmetric system, where the physical coil was mimicked by five coils with a pitch of 1.5 cm, an inner diameter of 6 mm, and an outer diameter 8 mm. However, this coil model does not exactly match the physical continuous coil with the aforementioned pitch and diameters. The simulation was run with currents and frequencies that are feasible for the power supply to generate. Fig. 2 shows the temperatures achieved by the COMSOL model after one hour of heating. Based on the model, temperatures needed to promote dissolution of the hydrogen into the α phase and, therefore, hydrogen extraction are attainable.

2.3. Stages and mass and energy balances

As was mentioned in the Introduction, the way in which the stages are meant to condense and capture lithium is based on the work done by Goldston [10,14] on the Lithium Vapor Divertor Box. The stages are held in excess of 320 °C in order to ensure that the lithium that is captured remains liquid. Eventually, outlets at these stages will be integrated into the design to divert clean lithium flow into a separate reservoir, which will be used as a holding tank for lithium that will be

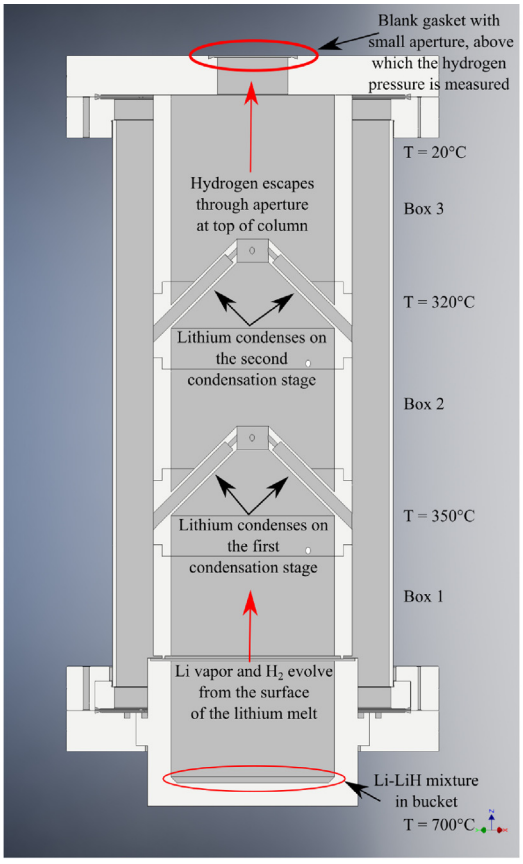

(a) Half-section view of the column body showing the stages angled upward at 45° and the slots allowing for hydrogen flow.

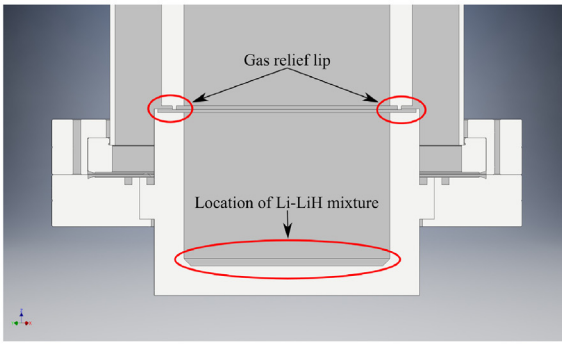

(b) A closeup half-section view of the lower column body. The bucket (lower) and main body (upper) are separated by a small gap, and a gas relief lip can be seen between the two sections.

Fig. 1. Section views of the column showing the main features: condensation stages, gas relief lip, nozzles for hydrogen flow, and the bucket for sample heating.

recycled back to the plasma-material interface.

While the addition of hydrogen increases the complexity of the system, the flux of lithium through each stage can be approximately modeled using the mass and enthalpy balances outlined by Goldston [10]. It should be made clear that this model is very approximate with regards to the system in this paper, but it can be used to estimate the amount of lithium that will condense on each stage. Assuming that the lithium flow through each stage aperture is defined by ideal-gas choked

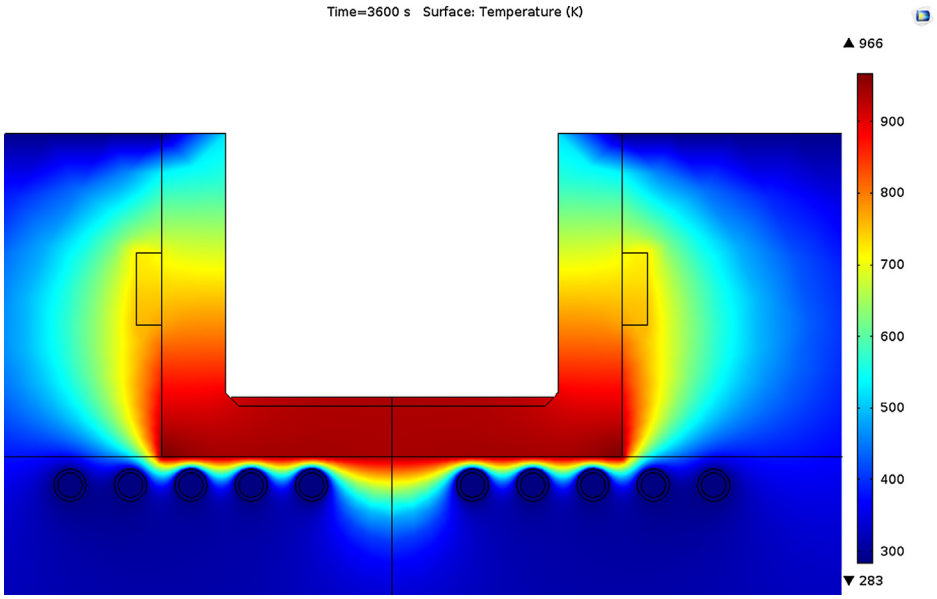

Fig. 2. Heat map of the bucket after 1 h at a current of 350 A and frequency of 30 kHz containing a sample of 6 g Li. The peak temperature is 966 K (693 °C) and the heat is spread evenly throughout the base of the bucket.

Table 1
Lithium properties within and flows out of each distillation column using Eqs. (5) and (6) and assuming no interaction with the hydrogen gas.

	A_{noz} [m^2]	A_{wall} [m^2]	T_{bot} [°C]	T_{top} [°C]	T_{vap} [°C]	n_{vap} [m^{-3}]	P [Torr]	$\dot{m}$ [g s^{-1}]
Box 1	2.29×10^{-4}	0.0546	700	350	2.47×10^{3}	6.30×10^{22}	6.09	1.10×10^{-1}
Box 2	2.29×10^{-4}	0.0417	350	320	4.94×10^{2}	1.20×10^{21}	9.51×10^{-2}	1.90×10^{-3}
Box 3	1.10×10^{-6}	0.0489	320	20	3.23×10^{2}	1.28×10^{20}	7.93×10^{-3}	8.63×10^{-7}

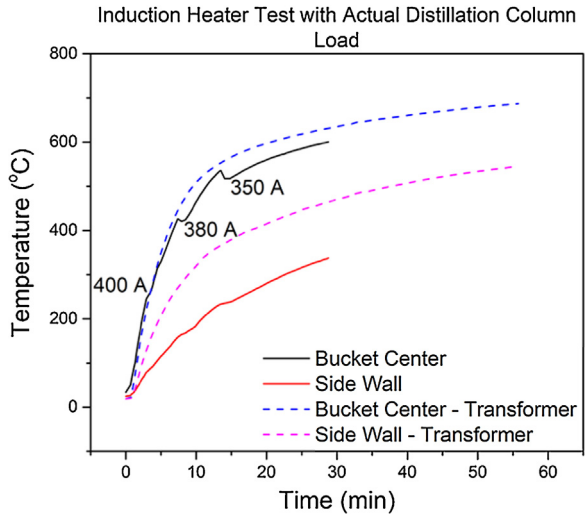

Fig. 3. Heating tests on the distillation column load with and without the transformer. The sudden drops in temperature seen in the test without the transformer show the tripping of the 20 A breaker. This was remedied by the ability of the step-down transformer to supply appropriate power. The dashed trends are those associated with the addition of the step-down transformer, while the solid lines indicate heating without this addition.

nozzle flow [10,15], and the lithium flux to and from the walls is defined by the Langmuir flux, then the following two relationships can be used [10]:

$$0.6288\sqrt{\frac{k}{m}}\left(A_{\mathrm{noz},i-1}n_{i-1}\sqrt{T_{\mathrm{vap},i-1}} - A_{\mathrm{noz},i}n_i\sqrt{T_{\mathrm{vap},i}}\right) + \sqrt{\frac{k}{2\pi m}}A_{\mathrm{wall},i}\left[n_{\mathrm{eq}}(T_{\mathrm{wall},i})\sqrt{T_{\mathrm{wall},i}} - n_i\sqrt{T_{\mathrm{vap},i}}\right] = 0, \quad (5)$$

$$0.62288\sqrt{\frac{k^3}{m}}\frac{5}{2}\left(T_{\mathrm{vap},i-1}A_{\mathrm{noz},i-1}n_{i-1}\sqrt{T_{\mathrm{vap},i-1}} - T_{\mathrm{vap},i}A_{\mathrm{noz},i}n_i\sqrt{T_{\mathrm{vap},i}}\right) + \sqrt{\frac{k^3}{2\pi m}}\frac{5}{2}A_{\mathrm{wall},i}\left[T_{\mathrm{wall},i}n_{\mathrm{eq}}(T_{\mathrm{wall},i})\sqrt{T_{\mathrm{wall},i}} - T_{\mathrm{vap},i}n_i\sqrt{T_{\mathrm{vap},i}}\right] = 0, \quad (6)$$

where k is Boltzmann's constant, m is the mass of lithium, A_{noz} is the cross-sectional area of the nozzle, A_{wall} is the accumulated area of the wall in each "box", n is the vapor number density, T_{vap} is the temperature of the vapor, T_{wall} is the temperature at the wall, and $n_{eq}(T_{wall})$ is the density defined by the lithium vapor pressure at T_{wall}. Knowing that there existed a temperature gradient between the bottom and top of each stage, Eqs. (5) and (6) were modified to include this effect. Table 1 lists the results from this evaluation, where the bottom temperature was 700 °C, the first stage was 350 °C, the second stage was 320 °C, and the exhaust aperture was set to room temperature.

3. Proof-of-concept results

Modeling of the induction heating system showed an achievable temperature very near the melting temperature of lithium hydride, so commissioning of the induction heating system began. After testing the efficacy of the heating system, two Proof-of-concepts experiments were performed to determine the column's ability to extract hydrogen from lithium melts of various saturation. A lithium-rich and lithium hydride-rich sample was used to determine the effect of hydrogen concentration on recovery rates. The way in which hydrogen evolution rates were measured for each of these Proof-of-concept tests will be explained in more detail in the following sub-sections.

3.1. Heater commissioning

Induction heating requires the use of a power supply and a copper coil for the generation of eddy currents in the workpiece. For the heating of the distillation column, the Dongguan HaiTuo Machinery Equipment Model HT-15A supply was chosen. The supply allows for control over the output current, has options for running in manual and automatic modes, and has a maximum power of 2.2 kW. OFHC copper was used to manufacture the five turn coil with an inductance close to the supplied coils. The inductance of the coil was determined to be 9μH by an LRC meter. To aid in the longevity of the supply, a water filtration system was put in place to cool the system along with decrease the buildup of contaminants in the supply.

Initial testing of the supply involved the heating of a 4.5″ stainless steel disk of 2.5″ in height. Achieving temperatures near 700 °C with this load led us to commence the heating of the column. Thermocouples placed in the center and outer wall of the bucket provide the melt temperature and the chamber temperature. The chamber temperature is used as an indication that heat is not transferring away from the column too rapidly. Initially, the power supply was receiving power from a 120 V 20 A circuit. However, this circuit could not produce the power needed to heat the bucket to the desired temperatures without tripping the breaker numerous times. In order to supply more power, a transformer was installed to step-down 208 V 1ϕ to 115 V 1ϕ. When the bucket was heated after the installation of the transformer, the power supply received its maximum power of 2.2 kW. Heating rates for tests with and without the transformer are seen in Fig. 3.

After an hour, the temperatures in the bucket reached a peak value of 687 °C. The temperature was still increasing at this time, leading to the conclusion that temperatures of 700 °C were attainable. The large disparity between the temperature of the bucket interior and exterior shows that heat transfer to the outer chamber occurs slowly enough to efficiently heat the bucket.

3.2. Li-rich vs. LiH-rich testing

An initial determination of the effect of hydrogen concentration on evolution rate was accomplished in two experiments: one with a Li-rich sample, and one with a LiH-rich sample. The distillation column was loaded into a drybox purged with argon. Since the only source of hydrogen in the sample was through the addition of LiH, the ratio of H/Li was determined by the mass of the lithium hydride powder and lithium granules contained in the sample. Inside the drybox, the sample was loaded into the bucket, and the bucket was attached to the chamber. The Li-rich sample contained a hydrogen molar ratio of 2 parts hydrogen to 100 parts lithium, while the LiH-rich sample contained a ratio of 80 parts hydrogen to 100 parts lithium. The chamber, packed with argon, was then connected to one turbomolecular pump and another section of chamber containing the RGA, full-range gauge, and a second turbomolecular pump. A rough pump was used to pump the outer

chamber sections, and, then, the column. The turbomolecular pumps were left to evacuate the chamber overnight to reach a base pressure of 5×10^{-7} Torr. The RGA section of chamber was differentially pumped because a pinhole aperture drilled into a blank copper gasket isolated it from the rest of the chamber.

The stages were preheated to 350 and 320 °C, for the first and second stage respectively, prior to turning on the induction power supply. A base scan of the system was taken using the RGA, which helped to identify the level of impurities that may have been in the lithium sample. The buildup of impurities was limited by loading in an inert environment and by "baking" the chamber to reduce the amount of water contained on the surfaces. The RGA tracked the partial pressures of: 1 AMU, 2 AMU, 6 AMU, 7 AMU, 18 AMU, and 28 AMU, over the duration of the test. The molecular hydrogen partial pressure for each sample was then converted to an evolution rate using the methodology described in the following paragraph. These rates were then used to compare how hydrogen concentration affects subsequent release. The bucket was heated for over an hour and the temperature of the lithium sample was recorded.

The partial pressure results for both the Li-rich and LiH-rich tests are shown in Fig. 4. While it looks as if both of these sample types are evolving similar amounts of hydrogen, it should be noted here that previous tests on LiH-rich samples were terminated prematurely because the amount of hydrogen registered by the RGA had saturated the filament. To combat this, a second pinhole aperture was added for the LiH-rich test only, and the system was calibrated using a controlled hydrogen inlet for both the Li-rich and LiH-rich arrangement. These calibrations were done separately for each sample type, where a known flow rate of hydrogen was introduced to the column at the location of where the sample was situated in the chamber. This hydrogen inlet setup replaced the bucket portion of the column during calibration. The RGA registered the partial pressures for the atomic and molecular hydrogen signals during calibration, where the amount of hydrogen introduced was increased in discrete steps. These pressures were compared to the precisely controlled flow rates, and a trend comparing pressure to flow rate was determined. Partial pressures from experimental runs were then converted to hydrogen flow rates using these calibration curves. Then, using the proper equation of state, the flow rates were converted to hydrogen particle evolution rates for both sample types, shown in Fig. 5. A comparison can now be drawn between the evolution rates of each sample type, which shows a significant difference in the amount of hydrogen that can be recovered between the two. This makes intuitive sense, since a higher hydrogen population in the sample enhances the probability that hydrogen atoms will recombine on the surface and release as H_2.

In both sample types, the hydrogen evolution rate reaches a peak (or a second peak) at temperatures ranging between 620 and 650 °C. This peak rate is preceded by a rapid increase in rate for temperatures in excess of 600 °C, which is important from a recovery point-of-view, since this will be the temperature range of interest. In each case, the rate then falls dramatically afterward, due to a substantial depletion of hydrogen in the sample. Essentially, recovery techniques that aim to use thermochemical treatment methods will need to focus on the temperature range between 600 and 650 °C.

One of the more peculiar results presented is the peak in the hydrogen evolution rate for the Li-rich sample, which occurs at approximately 400 °C. This peak is considered to be predominantly from the reaction which occurs between LiOH and LiH to produce H_2. Unfortunately, the loading procedure for this initial sample was not quite as rigorous as for the LiH-rich sample, as the dimensions of the original dry box used for loading prevented the insertion of the full column structure into the inert atmosphere chamber. As such, the bucket was loaded and quickly transferred under a continuous argon purge to the column body, which was held outside of the original dry box. This could have been a source for impurities, which would have been registered by the RGA as this type of signal. While it is likely that some LiH will dissolve into solution at these low temperatures and contribute, in part, to the signal peak observed at 400 °C, this contribution will be substantially less than the contribution from the reaction between LiOH and LiH. This is because of the way in which the samples were originally prepared, with the addition of pure LiH being the dominant source of hydrogen in the sample. As such, energy is required to break the Li-H bond and promote atomic hydrogen diffusion through the sample to the surface. It is at this surface that an atomic hydrogen will recombine with another to evolve as H_2. At temperatures near the observed 400 °C, the sample does not have sufficient energy to stimulate this process appreciably, so the source of the hydrogen signal observed at these temperatures is considered to be dominated by chemical interactions.

4. Discussion

Results from the Li-rich and LiH-rich samples indicate that the column is functioning as intended, with the stages being able to capture

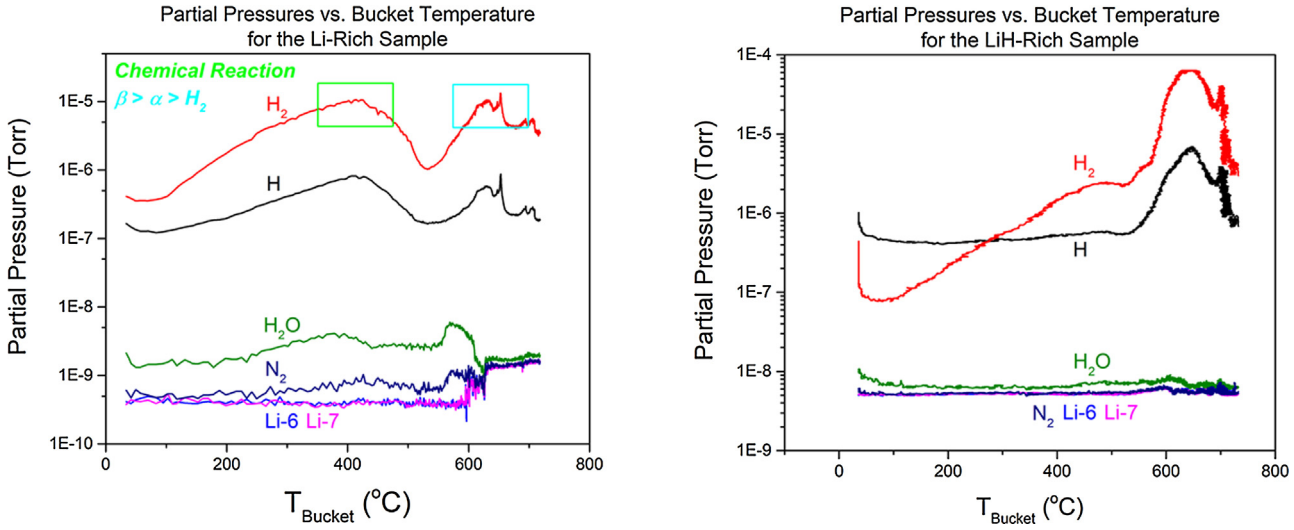

Fig. 4. (Left) The partial pressure plot for the Li-rich sample during the heating phase of the experiment. (Right) The partial pressure plot for the LiH-rich sample during the heating phase of the experiment. While it appears as if both samples are degassing the same amount of hydrogen, a second aperture was added for the LiH-rich test to protect the RGA filament from oversaturating, meaning the actual flow rate of hydrogen in the LiH-rich test is much greater than in the Li-rich test.

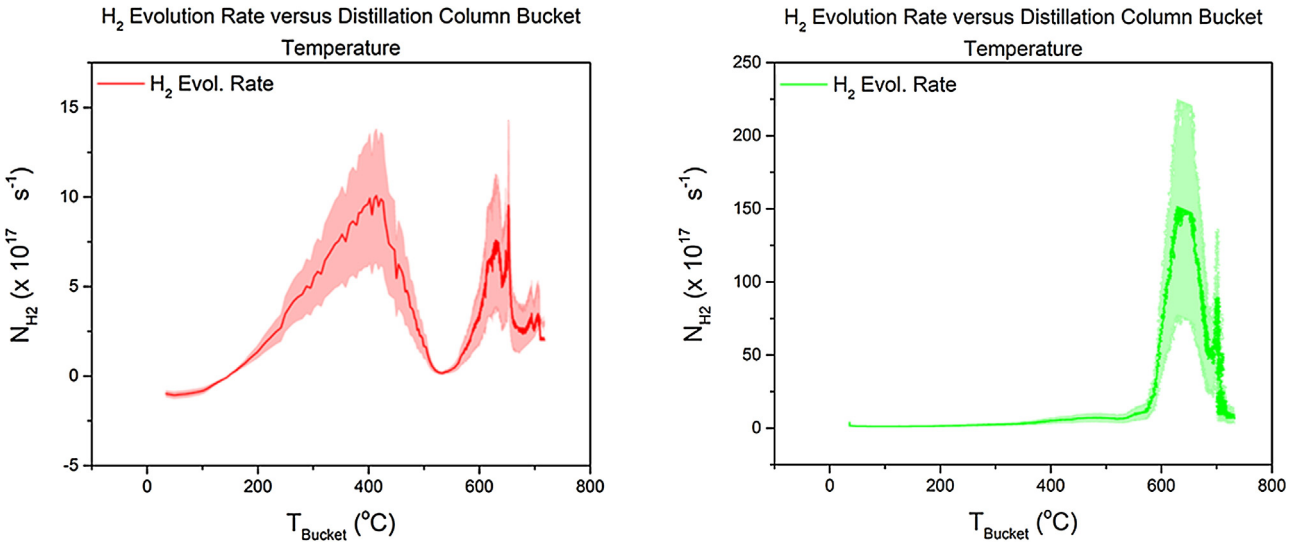

Fig. 5. (Left) The hydrogen evolution rate for the Li-rich test for the heating phase of the experiment. The first hydrogen peak is indicative of the reaction that occurs between LiOH and LiH to produce H_2, meaning impurities were present for this test. Thermal decomposition of LiH is the reason for the peak at higher temperatures. (Right) the hydrogen evolution rate for the LiH-rich test for the heating phase of the experiment. A comparison of the scale on each ordinate shows that the LiH-rich test is evolving substantially more hydrogen, albeit at higher temperatures.

and re-condense nearly all of the lithium, while large amounts of hydrogen were able to be quickly exhausted from the main chamber. Comparing the two sample types helps to prove the claim where LiH-rich solutions will evolve more hydrogen at faster rates, simply by virtue of the hydrogen population in solution, than will Li-rich solutions. This is important for thermal treatment efforts used to recover tritium, because these results help to solidify that separation technologies, such as those described by Ono [7] for his proposed liquid lithium loop, are necessary to recycle tritium fuel back to the reactor at rates that match or exceed in-vessel losses. More work needs to be done to investigate the ideal operating window of the distillation column described in this paper, as well as the state of the samples post-mortem; however, the initial results, and the models that support these results, are quite promising.

When considering the placement of this system within a fully-functional lithium loop, it is clear that this technology will be perfectly integrated into sections that were previously considered black boxes. This is especially true for each treatment method that defined tritium separation in terms of extracting lithium tritide from flowing lithium. While such methods may be able to extract the tritide salt, further treatment is necessary to recover tritium gas to be recycled as fuel, which is why technologies such as the column described in this paper are necessary. With regards to the loop system that Ono propose [7], this technology would be most applicable as the “Tritium Separator”. Assuming the induction heating power needed to promote tritium evolution scales linearly with surface area, the mass evolution rate described by Ono would require a column, or array of columns, with a power budget ranging in the 100s of kW to MW range. Alternative means of heating the column could also be used, such as diverting a portion of the reactor exhaust heat for this purpose.

The work done for the prototype column illustrates the importance of the hydrogen population within the sample; however, supplementary techniques can be added to the distillation column to promote tritium evolution in solutions with very low tritium mole ratios. In doing so, an optimization of these methods may yield tritium evolution rates that match in-vessel wall losses. One such technique that has proven to be promising in the fields of metallurgy and metal casting is ultrasonic degassing [8,16], whereby application of ultrasonic waves stimulates cavitation of gases trapped within solution. Under the right conditions, a net amount of gas will diffuse into the bubble causing it to grow, travel to the liquid surface, and rupture, releasing the captured gas. This type of technique, when used in tandem with heat and vacuum, has shown to be able to reduce the hydrogen content in liquid metals, with concentrations well below the solubility limits, by more than 50% [17]. A proper integration of this technology may help to broaden the operating window for the distillation column.

5. Conclusions

This paper described a prototype distillation column which can be used to recover hydrogen isotopes from liquid lithium in lithium-walled fusion systems. The uniqueness in the design of the column was described, and the induction heating capabilities were modeled using the COMSOL® Multiphysics software. A very simplified model was used to determine the lithium vapor characteristics between the condensation stages in the column, which will be verified in future work. Proof-of-concept tests were performed in the fully constructed prototype. A comparison was made between a Li-rich sample and a LiH-rich sample, where LiH was used in place of lithium deuteride (LiD) and lithium tritide (LiT) in each experiment. Results show that the hydrogen population in solution is critical to thermal recovery efforts, meaning separation technologies upstream of the column are recommended such that the column can be used to treat the LiD/LiT-rich solutions. The envisioned placement of this system in a fully-operational lithium loop was described. Future work will be used to flush out the optimal operating window for this technology, along with how supplementary recovery techniques may be suited to tritium recycling efforts.

Acknowledgments

This work was supported by the Department of Energy contract DE-SC0008587.

References

[1] G. Mazzitelli, M.L. Apicella, V. Pericoli Ridolfini, G. Apruzzese, R. De Angelis, D. Frigione, E. Giovannozzi, L. Gabellieri, G. Granucci, C. Mazzotta, M. Marinucci, A. Romano, O. Tudisco, A. Alekseyev, I. Ljublinski, A. Vertkov, Review of FTU results with the liquid lithium limiter, Fusion Eng. Des. 85 (6) (2010) 896–901 Proceedings of the 1st International Workshop on Lithium Applications for the Boundary Control in Fusion Devices.

[2] R. Majeski, S. Jardin, R. Kaita, T. Gray, P. Marfuta, J. Spaleta, J. Timberlake, L. Zakharov, G. Antar, R. Doerner, S. Luckhardt, R. Seraydarian, V. Soukhanovskii, R. Maingi, M. Finkenthal, D. Stutman, D. Rodgers, S. Angelini, Recent liquid lithium

limiter experiments in CDX-U, Nucl. Fusion 45 (6) (2005) 519.
[3] E. Joachim Roth, A. Tsitrone, Th. Loarte, G. Loarer, R. Counsell, V. Neu, S. Philipps, M. Brezinsek, P. Lehnen, Ch. Coad, K. Grisolia, K. Schmid, A. Krieger, B. Kallenbach, R. Lipschultz, R. Doerner, V. Causey, W. Alimov, O. Shu, A. Ogorodnikova, G. Kirschner, A. Federici, Kukushkin, Recent analysis of key plasma wall interactions issues for ITER, J. Nucl. Mater. 390–391 (2009) 1–9 Proceedings of the 18th International Conference on Plasma-Surface Interactions in Controlled Fusion Device.
[4] Y. Edao, S. Fukada, S. Yamaguchi, Y. Wu, H. Nakamura, Tritium removal by Y hot trap for purification of IFMIF Li target, Fusion Eng. Des. 85 (1) (2010) 53–57.
[5] E. Wakai, T. Kanemura, H. Kondo, Y. Hirakawa, Y. Ito, H. Serizawa, Y. Kawahito, T. Higashi, A. Suzuki, S. Fukada, K. Furuya, K. Esaki, J. Yagi, Y. Tsuji, T. Ito, S. Niitsuma, S. Yoshihashi-Suzuki, K. Watanabe, T. Furukawa, F. Groeschel, G. Micciche, S. Manorri, P. Favuzza, F.S. Nitti, R. Heidinger, T. Terai, H. Horiike, M. Sugimoto, S. Ohira, J. Knaster, Engineering validation for lithium target facility of the IFMIF under IFMIF/EVEDA project, Nucl. Mater. Energy 9 (2016) 278–285 cited By 1.
[6] H. Moriyama, S. Tanaka, D.K. Sze, J. Reimann, A. Terlain, Tritium recovery from liquid metals, Fusion Eng. Des. 28 (C) (1995) 226–239 cited By 51.
[7] M. Ono, R. Majeski, M.A. Jaworski, Y. Hirooka, R. Kaita, T.K. Gray, R. Maingi, C.H. Skinner, M. Christenson, D.N. Ruzic, Liquid lithium loop system to solve challenging technology issues for fusion power plant, Nucl. Fusion 57 (11) (2017) 116056.
[8] Michael Christenson, The Design and Development of Hydrogen Isotope Extraction Technologies for a LiMIT-Style Liquid Lithium Loop (Ph.D. thesis), University of Illinois at Urbana-Champaign, Champaign, IL, 2018.
[9] COMSOL, COMSOL Multiphysics Reference Manual, 4.4. ed., (2013 November).
[10] R.J. Goldston, R. Myers, J. Schwartz, The lithium vapor box divertor, Phys. Scripta 2016 (T167) (2016) 014017.
[11] A.B. Martin-Rojo, E. Oyarzabal, T.W. Morgan, F.L. Tabarés, Exposure of liquid lithium confined in a capillary structure to high plasma fluxes in pilot-psi – influence of temperature on D retention, Fusion Eng. Des. 117 (2017) 222–225.
[12] M.J. Baldwin, R.P. Doerner, R. Causey, S.C. Luckhardt, R.W. Conn, Recombination of deuterium atoms on the surface of molten Li-LiD, J. Nucl. Mater. 306 (1) (2002) 15–20.
[13] M.J. Baldwin, R.P. Doerner, S.C. Luckhardt, R.W. Conn, Deuterium retention in liquid lithium, Nucl. Fusion 42 (11) (2002) 1318.
[14] R.J. Goldston, A. Hakim, G.W. Hammett, M.A. Jaworski, J. Schwartz, Recent advances towards a lithium vapor box divertor, Nucl. Mater. Energy 12 (2017) 1118–1121 Proceedings of the 22nd International Conference on Plasma Surface Interactions 2016, 22nd PSI.
[15] Y.A. Çengel, J.M. Cimbala, Fluid Mechanics: Fundamentals and Applications. McGraw-Hill Series in Mechanical Engineering, McGraw-Hill Higher Education, 2006.
[16] A.R. Naji Meidani, M. Hasan, A study of hydrogen bubble growth during ultrasonic degassing of Al–Cu alloy melts, J. Mater. Process. Technol. 147 (3) (2004) 311–320.
[17] H. Xu, Q. Han, T.T. Meek, Effects of ultrasonic vibration on degassing of aluminum alloys, Mater. Sci. Eng. A 473 (1) (2008) 96–104.